A Surface Micromachined Optical Scanner Array Using Photoresist Lenses Fabricated by a Thermal Reflow Process

Hiroshi Toshiyoshi, *Member, IEEE*, Guo-Dung John Su, *Member, IEEE*, Jason LaCosse, *Member, OSA*, and Ming C. Wu, *Fellow, IEEE, Member, OSA*

***Abstract*—This paper presents the design, fabrication, and operation of a newly developed micromechanical optical scanner array using a translating microlens. We have used photoresist reflow techinique to form a microlens on a surface micromachined XY-stage of the scratch-drive actuation mechanism. The lens scanner is placed at the focal length from an incident optical fiber to collimate the transmitting light. The collimated beam is steered two-dimensionally by the XY-motion of the microlens with respect to the incident fiber. We also have developed a theoretical model to predict appropriate initial resist thickness and diameter for the scanning lens. An optical scanning angle of $\pm 7^\circ$ has been demonstrated by sliding a microlens of 670-μm focal length at a physical stroke of ± 67 μm. Typical angular positioning resolution has been estimated to be 0.018°.**

***Index Terms*—Microactuator, microlens, optical scanner, photoresist reflow technique, XY-stage.**

I. Introduction

OPTICAL switching devices for all-optical fiber network are under intensive development because of the increasing demand for higher data-traffic rates. In particular, optical cross-connectors (OXCs) and add/drop multiplexers (ADMs) of large port count are the key components that dominate the traffic capacity and the network flexibility of the wavelength-division multiplexing (WDM) systems. Requirements for those devices are, for example, minimum insertion loss, low return loss, small crosstalk between channels, small polarization-dependent loss, scalability to larger input and output port count, and low production cost. Optical microelectromechanical systems (MEMS) approach [1]–[4] falls into this request better than the approaches using massive switching boards of solid-state devices based on optoelectro (OE) and electroopto (EO) conversions.

Today's optical MEMS research is focusing on the development of micromirror arrays of large optical angle, of low driving voltage, and for larger port counts [5]–[7]. Fig. 1(a) illustrates the use of a micromirror, which steers the incident light from a fiber collimator to any one of the output scanning mirrors to complete an optical route. In fact, the most significant components in the system are the fiber collimators. The intensity beam profile and aberration affect the insertion loss of the whole system, and collimation distance determines the maximum number of channels that can be addressed with an acceptable coupling loss. Collimators are often used in the form of an $N \times N$ array of microlenses with its pitch matching that of an $N \times N$ optical fiber bundle. These two pieces should be in perfect alignment to guide parallel collimated beams straight down to the micromirror arrays.

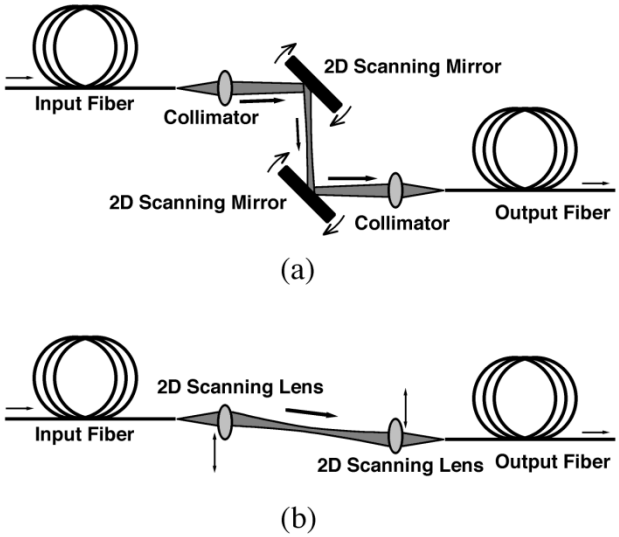

Fig. 1. Principles of micromechanical optical switches using (a) tilting mirrors and (b) sliding lenses.

Here we need to take the deviation of the fiber core position into account, which is usually ± 0.5 to 1 μm with respect to the true center of the fiber diameter. Alignment errors in assembling fiber bundles of around ± 0.5 μm would be added to give a total deviation of 1–1.5 μm. The relative displacement between the core and the lens causes an angular offset in the direction of the collimated beam, and then it is translated to the displacement of the beam position on the micromirror unit. Provided that the focal length of the microlens is 1 mm and the travelling distance from the lens to the mirror is 30 mm, the spot shift is calculated to be 45 μm. Therefore, one may need to design mirrors larger than the actual beam spot in order to absorb the walkoff of the beam spot. Furthermore, the offset affects the insertion loss of

Manuscript received April 9, 2003. This work was supported in part by the Micromachine Center, Japan, under a Research Grant and by the Japan Ministry of Education, Culture, Sports, Science and Technology under an Overseas Study Subsidy.

H. Toshiyoshi is with the Institute of Industrial Science, University of Tokyo, 153-8505 Tokyo, Japan.

G.-D. J. Su, J. LaCosse, and M. C. Wu are with the University of California Los Angeles, Los Angeles, CA 90024 USA (e-mail: hiro@iis.u-tokyo.ac.jp).

Digital Object Identifier 10.1109/JLT.2003.814399

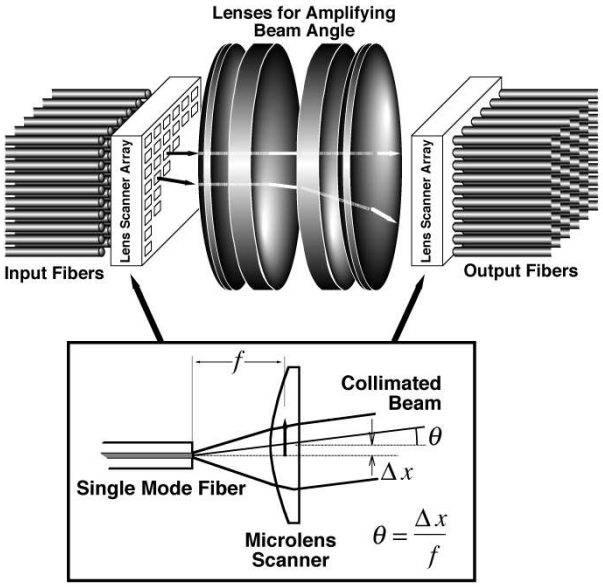

Fig. 2. Schematic view of MEMS OXC using 2-D microlens scanner array. Collimated beam from each fiber is steered by the lens scanner to any one of the output fibers. Telescope lenses are optional for amplifying scan angle.

the entire system as well as the uniformity of the optical performance of channels.

In this paper, we propose an alternative method of steering light beams by using microlenses instead of micromirrors. A photoresist reflow lens has been mounted on a surface micromachined XY-scanning stage, and two-dimensional (2-D) scanning of infrared light has been demonstrated to achieve maximum steering angle of $\pm 7^{\circ}$. A theoretical model of designing a photoresist microlens has been developed in good agreement with experimental results. The reliability issue related to the surface friction of a polysilicon micromechanism is discussed.

II. MEMS 2-D Microlens Scanner

A laterally scanned microlens is able to absorb the fiber core deviation by finely tuning the lens position with submicrometer accuracy. It also can steer a collimated beam with a large angle when the lens is moved with a large stroke [8]. Microlens scanners can be used as an optical switching element in place of scanning mirrors [9], as schematically illustrated in Fig. 1(b). It is also possible to use an array of such lens scanners to compose a larger matrix switch, as shown in Fig. 2. Input lights are guided through the fiber bundles located on the left-hand side of the system. Each fiber has a 2-D lens scanner such that the transmitting light can be individually steered to any one of the output ports located on the right-hand side of the figure. As shown in the figure's inset, a microlens is located at the focal length from a point light source (fiber facet) and collimates the beam. It is also possible to form a beam waist in the optical path, as shown in Fig. 1(b), by slightly displacing the lens away from the fiber. Neglecting this small displacement, one can write the beam steering angle as $\Delta x/f$, where f is the focal length of the lens and Δx is the transversal displacement of the lens. In this schematic, a pair of telescopes is shown as an option to amplify the steering angle of the travelling light [8].

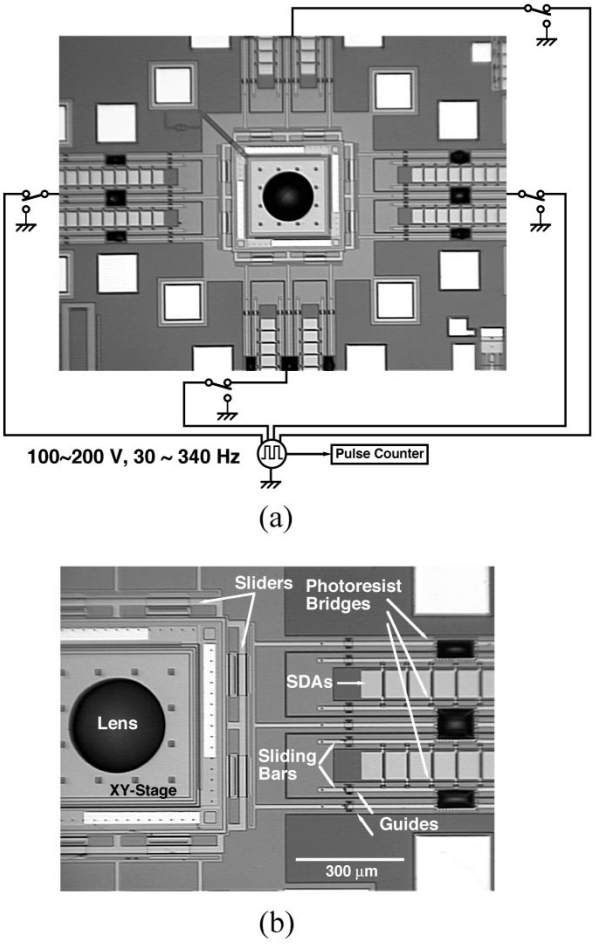

Fig. 3. Photographs of polysilicon surface micromachined 2-D lens scanner. (a) Entire view and (b) closeup view of the XY-stage. The lens and the fixing bridges are made by photoresist reflow technique.

The XY-stage for scanning the microlens has been fabricated by using an external MEMS foundry, multiuser MEMS processes (MUMPs), of Cronos,[1] and the microlens has been postprocessed in-house by using the photoresist reflow technique [10]–[12]. Fig. 3(a) shows part of a 2×2 lens scanner array. A closeup view of the microlens and actuators is shown in Fig. 3(b). A photoresist microlens (diameter 260 μm) is sitting on a suspended polysilicon diaphragm of 500×500 μm^2 in area and 1.5 μm in thickness. There is no hole as an optical aperture in the diaphragm or in the silicon substrate because silicon is transparent for infrared light of 1.55-μm wavelength.

Independent X- and Y-motion is possible by using a pair of sliders attached on the edges of the stage. The stage is pulled by four sets of scratch-drive actuator (SDA) arrays [13], whose bidirectional motion is guided by the staple guides over the sliding bars. Driving voltages are supplied from the peripheral contact pads through the SDAs' bushings. Three islands of photoresist bridges next to the SDA arrays provide mechanical connection and electrical isolation between the XY-stage and the SDAs [14].

[1]http://www.memsrus.com/cronos/.

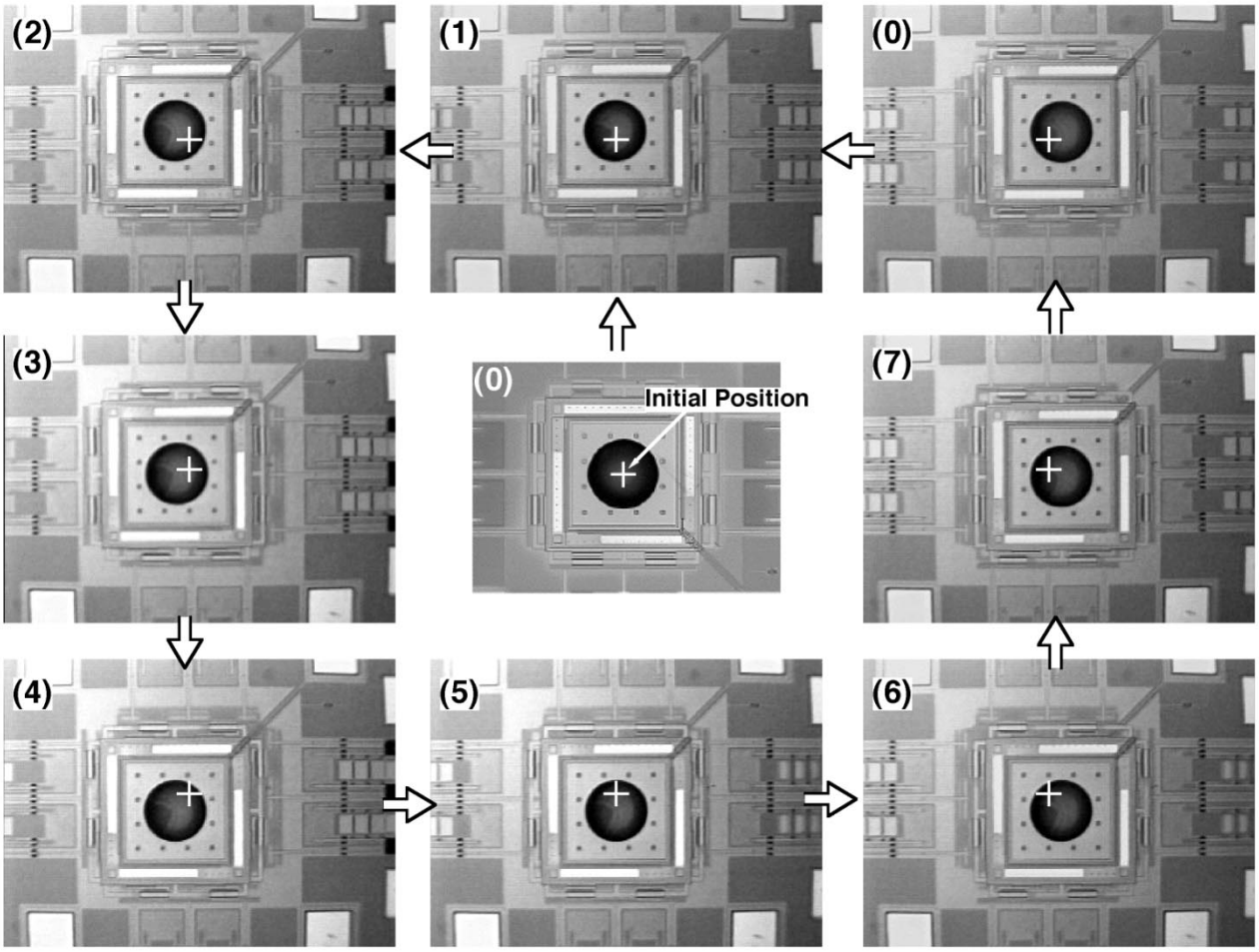

Fig. 4. Snapshots of microlens scanner in 2-D motion.

Fig. 4 shows microscope snapshots of the lens scanner actuated in the X- and Y-directions. The initial center position of the lens is shown by a white cross. Maximum displacement is limited to ± 67 μm, which is the stroke allowed by the coupling sliders. The detailed structure of the slider will be shown in Section V. The lens position is controlled by counting the total pulse numbers of voltages applied to the SDA arrays. The average number of pulses needed for the slider to travel from one end to the other (approximately 130-μm stroke) has been found to be 400 pulses with a square voltage of $200V_{\rm peak}$ at 340 Hz. Positioning resolution is thus estimated to be 0.33 μm per pulse. Faster actuation is possible, but this frequency has been chosen to achieve the most smooth motion of the slider. While the slider is moving by one set of SDA arrays, no voltage is applied to the other three sets of SDAs.

A simplified process of lens scanner fabrication is shown in Fig. 5. In step (1), the backside surface of the MUMPs chip (1 cm $\times$ 1 cm) is polished to a mirror surface in order to minimize optical diffraction of the transmitting light. In (2), a thick photoresist (Hoechst AZ-4620) is spun on the front surface, and a circular pattern is formed on the XY-stage. The typical initial thickness of the resist is 10 μm, as discussed in Section III. To suppress the photoresist edge-beads, we have prepared dummy chips of the same thickness as the MUMPs chip and tiled them together on a carrier wafer before spincoating. A diluted developer [100-ml AZ-400 K with 100-ml deionized water (DIW)] is used for development for 1 min. In (3), the circular photoresist pattern is thermally transformed into a spherical microlens by baking on a 150 °C hotplate for 1 min. The resist patterns can be visually observed half-melting under the microscope. Baking longer than 1 min should be avoided, as it frequently led to bubble-forming in the microlens. The sacrificial phosphosilicate glass (PSG) layers are removed in a concentrated hydrofluoric acid (47%) at room temperature for 10 min, followed by two cycles of 30-min rinse in DIW warmed at 60 °C. The chip is dried at room temperature without using any organic solvent replacement to avoid damaging the photoresist microlens. In spite of the large area of the XY-stage, no serious sticking problem has been observed thanks to the stage height (over 20 μm) elevated by the stress-induced polysilicon-metal cantilevers [15], as depicted in Fig. 5 In (4), there is an auxiliary polysilicon electrode beneath the XY-stage for the focusing control ability, which is not used in our experiment.

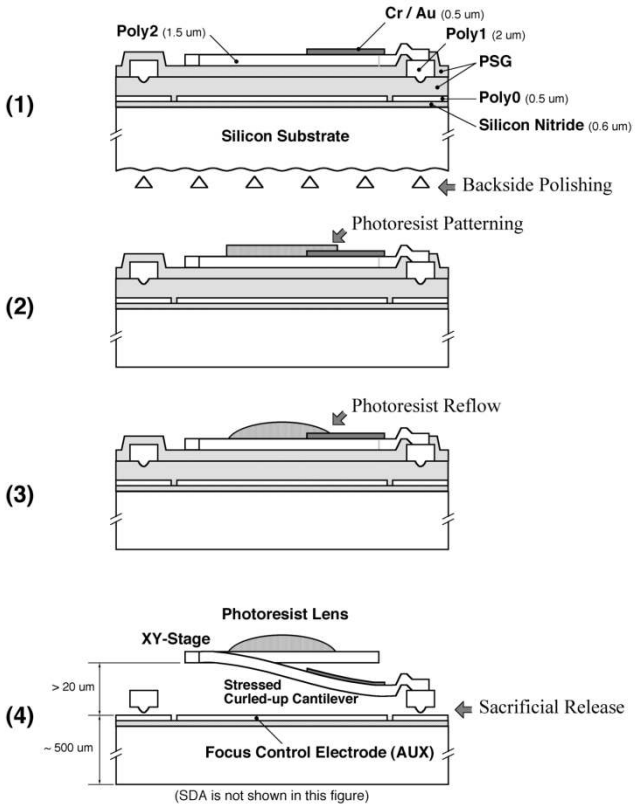

Fig. 5. Fabrication process of making photoresist reflow lens on MEMS XY-stage.

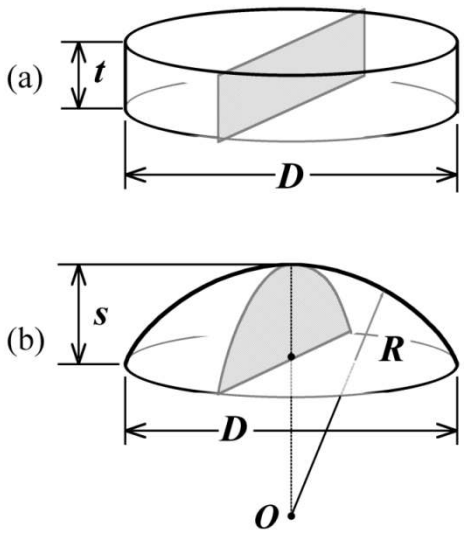

Fig. 6. Photoresist pattern (a) before and (b) after reflowing process.

III. Photoresist Lens Design

The photoresist pattern before reflow is in a column shape of height t and diameter D, as shown in Fig. 6(a), and its volume is

$$V_{\text{initial}} = \frac{\pi}{4} D^2 t. \tag{1}$$

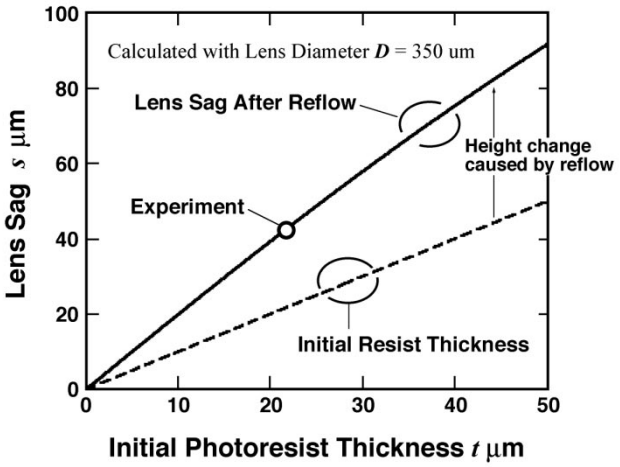

Fig. 7. Calculated lens sag as a function of the initial photoresist thickness (for lens diameter of 350 μm).

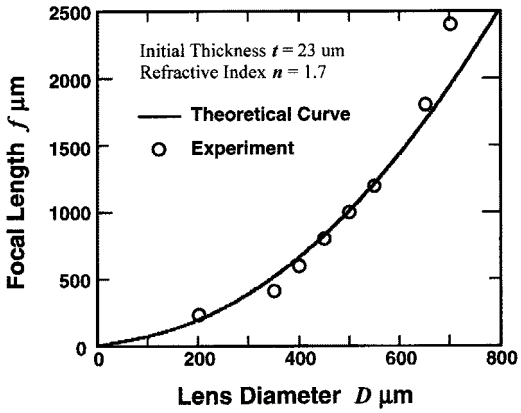

Fig. 8. Calculated focal length and experimentally obtained results as a function of lens diameter. Initial resist thickness has been set to 23 μm.

We have observed that the resist pattern reflows without changing the footprint diameter. By scanning the exact center line of each photoresist pattern with a contact-type surface profile measurement (Dektak-8 Profilometer), we have experimentally conformed that the resist pattern has turned into a spherical shape as shown in Fig. 6(b). The radius of lens curvature is written as

$$R = \frac{s}{2} + \frac{D^2}{8 \cdot s} \tag{2}$$

where s is the lens sag. Therefore, the volume of the plano-convex lens is

$$V_{\text{lens}} = \pi \int_{R-s}^{R} \left(R^2 - y^2\right)\, dy = \frac{\pi s}{24}\left(3D^2 + 4s^2\right). \tag{3}$$

Neglecting the volume change before and after thermal reflow, we equalize (1) and (3) to find the lens sag as a function of D and t as

$$s = s(t, D) = A - \frac{1}{4}\frac{D^2}{A} \tag{4}$$

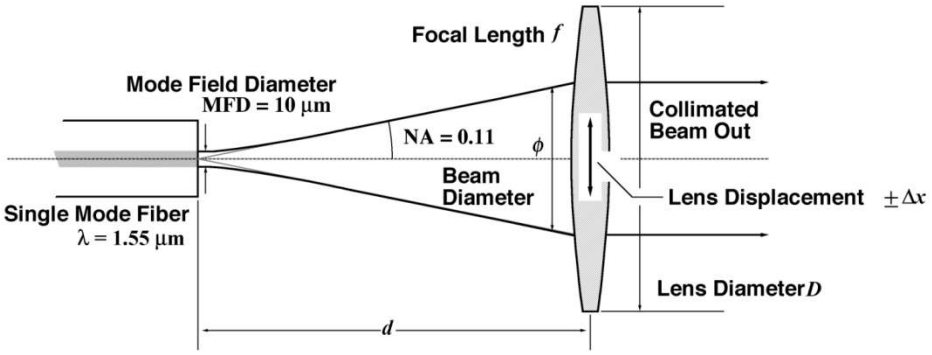

Fig. 9. Analytical model for calculating the beam diameter at the lens.

where

$$A \equiv \left(\frac{3}{4}t\,D^{\,2} + \frac{1}{8}\sqrt{D^{\,6} + 36\,t^{\,2}D^{\,4}}\right)^{1/3}. \qquad (5)$$

Using a value of 350 μm for D, we plot lens sag as a function of the initial resist thickness in Fig. 7. It is clearly seen that the lens sag is almost double the initial thickness, which agreed well with our experimentally observed values (circular dot in Fig. 7) showing an initial value of 11 μm and a lens sag of 23 μm after reflow.

The focal length of a plano-convex lens is $R/(n-1)$, where n is the refractive index of the lens material. Substituing (2), (4), and (5) into this, one obtains a formula of focal length as

$$f = f\,(t,\ D) = \frac{1}{n-1}\left\{\frac{s\ (t,D)}{2} + \frac{D^{\,2}}{8\,s\ (t,D)}\right\}. \qquad (6)$$

The focal length of a photoresist reflow lens is thus controlled by the initial resist thickness t and the dimension of mask pattern D.

To find a value of n as a fitting parameter, we have prepared microlenses of various diameters ranging from 200 to 800 μm at the identical initial resist thickness of 23 μm (Hoechst AZ-4620 double-spun at 2000 rpm for 30 s). The resist patterns are reflowed by the technique described in the previous section. To determine focal length, we set a single-mode fiber with its facet facing the convex surface of the microlens and observed a beam spot of an infrared 1.55-μm-wavelength light on a sensor card placed 1 m behind the microlens. In our experiment, the focal length has been defined by the distance between the fiber facet and the lens surface when a beam spot was collimated. Fig. 8 plots the focal length as a function of lens diameter. The distribution of the experimental data could be well explained by the theoretical model when using the refractive index of 1.7 as a fitting parameter.

Let us now use (6) and $n = 1.7$ to find the optimal design of the microlens. As illustrated in Fig. 9, the beam emitted from a single-mode fiber can be modeled by the Gaussian theory at far field. Setting a beam waist at the fiber facet, we write the spot diameter measured on the microlens as

$$\begin{cases} \phi = \frac{2\lambda d}{\pi w_0} \\ w_0 = \frac{\mathrm{MFD}}{2} \end{cases} \qquad (7)$$

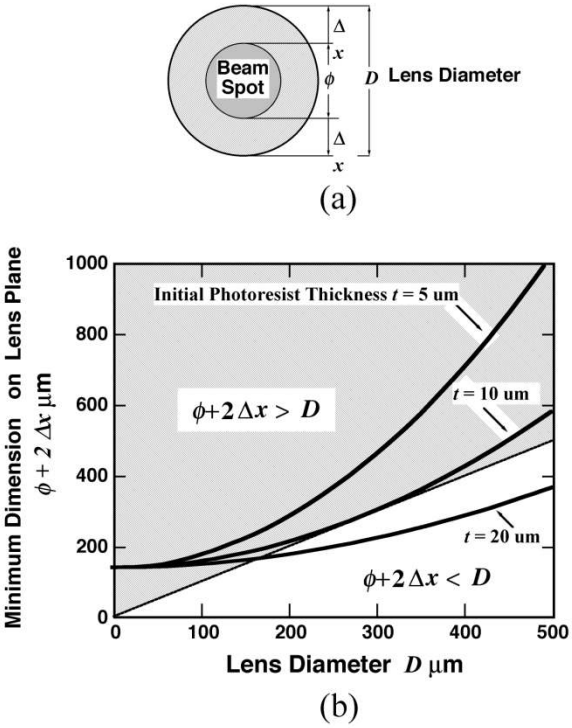

Fig. 10. (a) Lens diameter should be larger than the beam spot and displacement margin. (b) Minimum dimension for lens scanner as a function of lens diameter. Hatched area shows impractical dimensions.

where MFD is the mode field diameter of single-mode fiber (10 μm). The distance d is set to be the focal length of the lens $f(t,D)$ in order to collimate the light. For optical scanning, the beam spot diameter should be smaller than the lens diameter to avoid losing optical energy. Furthermore, lens displacement Δx should be taken into account as a margin shown in Fig. 10(a). The criteria for optical design is written, therefore, as

$$\phi(t,D) + 2\Delta x < D. \qquad (8)$$

Fig. 10(b) plots values of $\phi + 2\Delta x$ as a function of lens diameter, where Δx is set to 67 μm for our XY-stage design. Three curves are shown at different initial resist thicknesses of 5, 10, and 20 μm. As seen in the plot, the 5-μm-thick photoresist is too thin to fulfil the criteria in (8) because the entire curve is in

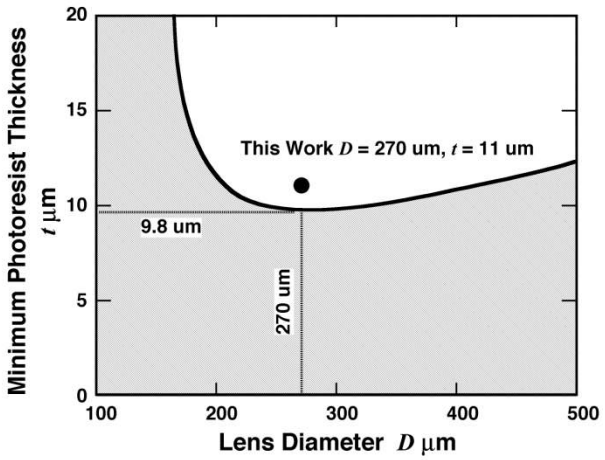

Fig. 11. Minimum initial thickness of photoresist as a function of lens diameter. Hatched area shows impractical dimensions.

the hatched area, where $\phi + 2\Delta x$ is greater than D. On the other hand, the 20-μm-thick photoresist is good for lens diameter of 160 μm or larger. The critical value of t for satisfying (8) has been found to be 9.8 μm.

We define the minimum resist thickness by using the smallest value of t that fulfils (8) under a given lens diameter D. Fig. 11 shows such minimum thickness as a function of lens diameter. The lens dimensions in the hatched area cannot be realized due to the optical design constraint. Again, no reflow lens can be made with photoresist thinner than 9.8 μm. From a photolithographic point of view, photoresist should be as thin as possible to keep high resolution in patterning. Therefore, we used a lens diameter of 270 μm on the photomask and a resist thickness of 11 μm, which is indicated by the dot just above the boundary in Fig. 11. The target focal length was set to be 610 μm to achieve more than $\pm 6^\circ$ beam-steering angle with the maximum lens displacement of 67 μm. The actual focal length was measured to be 670 μm, which was found to be longer than the designed value possibly because the photoresist had been thinned during development. Good reproducibility of focal length was observed throughout our experiment.

IV. Beam Steering

For testing optical scanning performance, we mounted the chip on a printed circuit board (PCB) with a tiny hole in the middle as an optical aperture, and finished electrical interconnetion to the XY-stages by bonding gold wires. The PCB was fixed vertically on a modified lens holder of five degrees of freedom in position alignment, as shown in Fig. 12(a). A single-mode fiber was placed in front of the microlens, as illustrated in Fig. 12(b), by using a microscope for visually controlling the fiber position. A collimated beam spot after the lens was observed at an 8-cm distance by using an infrared charge-coupled device (CCD) camera (Hamamatsu Photonics, model C2400–03).

Fig. 13 shows CCD images of displaced beam spot. Maximum spot displacement of more than ± 10 mm on the CCD image plane was obtained, which corresponded to a scan angle

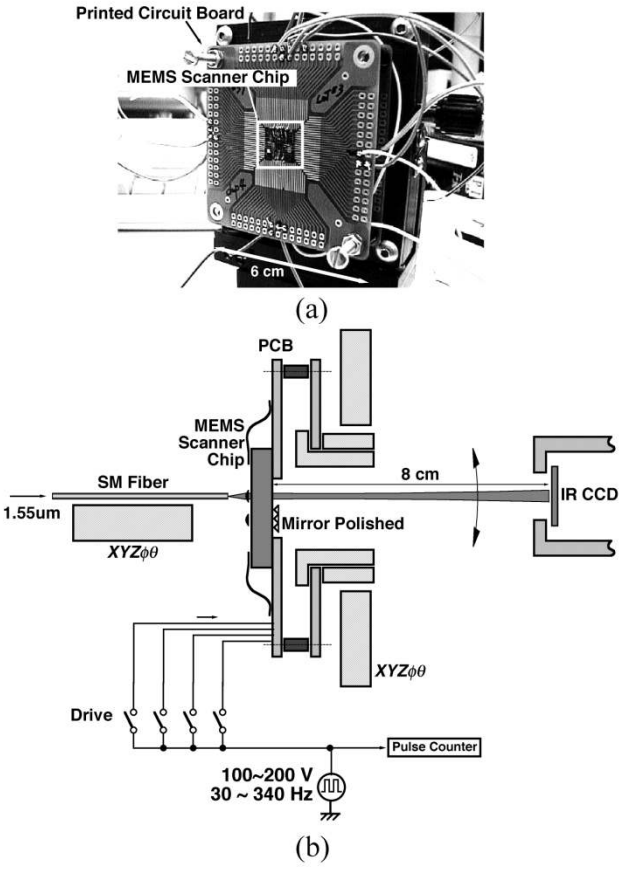

Fig. 12. (a) Lens scanner chip mounted on a printed circuit board for optical test and (b) schematic view of the apparatus arrangement.

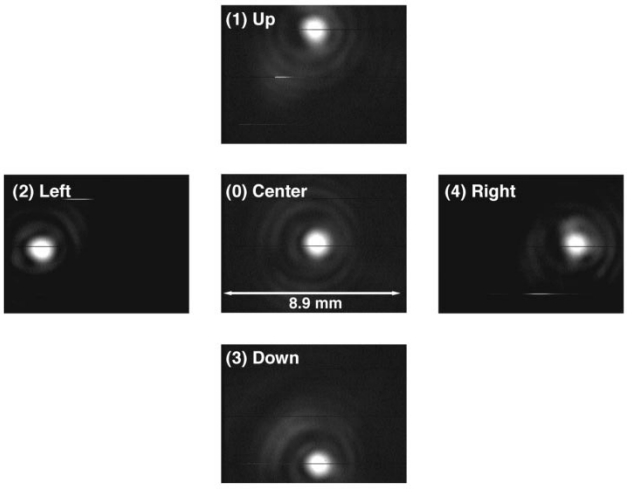

Fig. 13. Infrared CCD images of 2-D steered beam spot. Scan angle of $\pm 7^\circ$ is larger than the image plane of the CCD.

of more than $\pm 7^\circ$. Angular resolution is estimated to be 0.018° because it took approximately 400 pulses of driving voltage for the full stroke. Unlike typical electrostatic or thermal scanning mirrors [16], the lens scanner can be latched at any place without applying voltage thanks to the friction between the sliding bar and the staple guides. The beam spot was found to be accompanied with several coaxial rings due to the optical interference

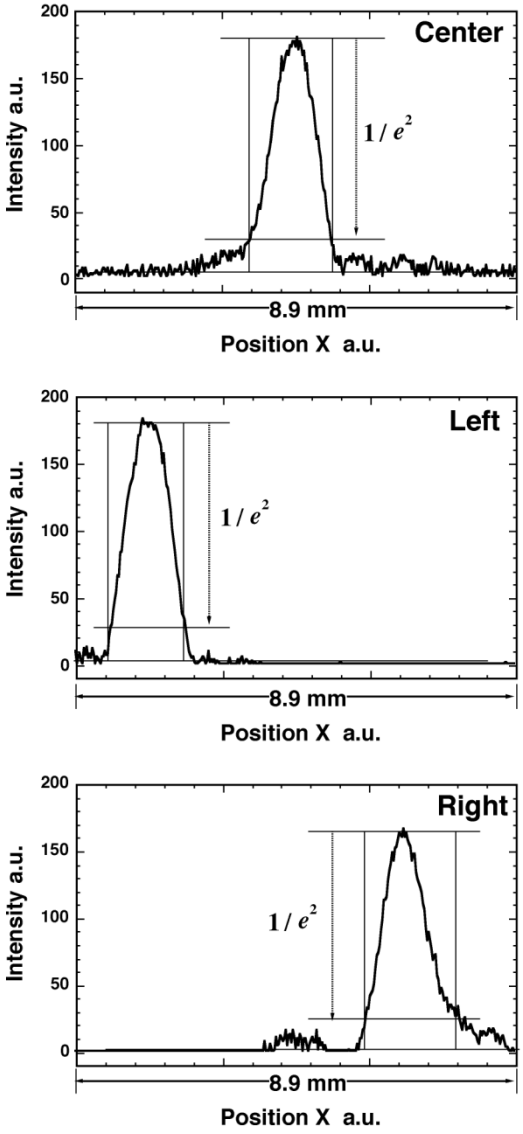

Fig. 14. Intensity profiles of steered beam spot measured at center, left-hand-side, and right-hand-side positions.

in the multiple interfaces of MUMPs layers (see Fig. 5). The interference can be suppressed by using simpler layer structure and by removing the silicon substrate in the optical path. The intensity profile of the steered beam is shown in Fig. 14. The beam at the rest position (center) can fit well to the squared Gaussian profile. No significant intensity change or spot size change could be observed to scan angles up to 5°. For larger scan angles, the beam starts to show deviation from the Gaussian profile.

V. Slider Reliability Issue

Several different types of MEMS XY-stages have been tested in our experiment to investigate the reliability of microfriction at the slider part. In our prototype model, photoresist fixing bridges were placed close to the slider as shown in the scanning electron microscope image in Fig. 15(a). The slider plates should be as flat as possible so as not to cause friction on the sliding parts nested with each other. However, the residual stress

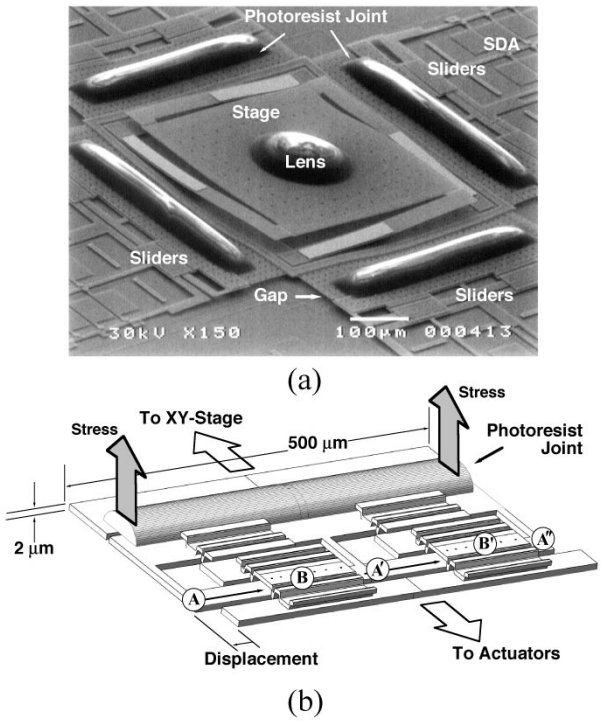

Fig. 15. (a) Prototype design of scanning lens. Photoresist fixing bridges are located close to the sliders. (b) Schematic illustration of the slider parts.

of photoresist had buckled up the joining plates. A relatively large gap can be seen under the edge of the plates. In addition, the bottom surface of the photoresist lens is no more flat but slightly round due to the warp of the stage plate.

Deformation of the sliding plates [section A-A'-A" in Fig. 15(b)] has been observed with the confocal interferometric microscope, and its surface profile is shown in Fig. 16(a). The two bumps are the overhanging bridges B and B'. Due to the residual stress of photoresist, peak-to-valley deflection was as large as 4.6 μm across a 500-μm-long plate. Because the gap clearance between the sliding plates was less than 1 μm, the slider suffered from the friction, and stick-and-slip motion of the stage was frequently observed even with a large array of SDAs (4×6 plates). In our later design, the photoresist fixing bridges and joining plates have been relocated far from the sliders, as shown in Fig. 3(b). The surface profile of the improved slider is shown in Fig. 16(b). The peak-to-valley deflection has been decreased to 0.5 μm, which remains due to the polysilicon's intrinsic stress. We could observe smoother motion of the XY-stage of this slider design even with a smaller array of SDAs (2×10 plates).

VI. Summary

A newly developed surface micromachined lens scanner has been presented, and an optical scanning angle of $\pm 7°$ has been demonstrated with a 1.55-μm-wavelength infrared light. The lens stage is made of a polysilicon surface micromachined XY-stage of two degrees of motion freedom. Scratch-drive actuators and decoupling sliders have been used as a 2-D actuation mechanism. The microlens has been prepared by

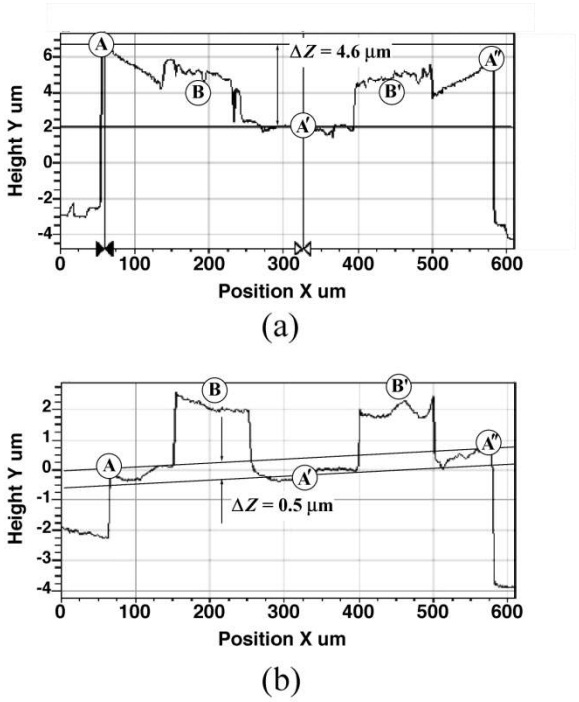

Fig. 16. Surface profiles showing (a) buckled slider plates of the prototype design [Fig. 15(a)] and (b) flat slider plates of the improved design [Fig. 3].

using the photoresist reflow technique. A theoretical optomechanical model of the lens scanner has been developed to appropriately design the dimension of the photoresist reflow lens. The reliability of the micromechanical sliders has been studied, and a stage design for smooth XY-motion has been presented. Thanks to the latching capability, the lens scanners can be used as a position tunable collimator array as well as a switching element of optical crossconnectors.

REFERENCES

[1] L. Y. Lin, E. L. Goldstein, and R. W. Tkach, "Free-space micromachined optical switches for optical networking," *IEEE J. Select. Topics Quantum Electron.*, vol. 5, no. 1, pp. 4–9, 1999.

[2] M. C. Wu, L. Fan, and G.-D. Su, "Micromechanical photonic integrated circuits," *Trans. IEICE*, vol. E83-C, no. 6, p. 903, 2000.

[3] F. Fujita and H. Toshiyoshi, "Micro-optical devices," in *A Chapter Contributed to P. Rai-Choudhury: Handbook of Microlithography, Micromachining*. Bellingham, WA: SPIE Optical Engineering Press, 1997.

[4] J. A. Walker, "The future of MEMS in telecommunications networks," *J. Micromech. Microeng.*, vol. 10, no. 3, pp. R1–R7, Sept. 2000.

[5] D. T. Neilson, V. A. Aksyuk, S. Arney, N. R. Basavanhally, K. S. Bhalla, D. J. Bishop, B. A. Boie, C. A. Bolle, J. V. Gates, A. M. Gottlieb, J. P. Hickey, N. A. Jackman, P. R. Kolodner, S. K. Korotky, B. Mikkelsen, F. Pardo, G. Raybon, R. Ruel, R. E. Scotti, T. W. Van Blarcum, L. Zhang, and C. R. Giles, "Fully provisioned 112 × 112 micro-mechanical optical crossconnect with 35.8 Tb/s demonstrated capacity," in *Proc. 25th Optical Fiber Commun. Conf. (OFC'2000)*, Baltimore, MD, Mar. 7–10, 2000, PD12-1.

[6] V. A. Aksyuk, "Beam steering micromirrors for optical telecommunication," in *Proc. IEEE/LEOS Int. Conf. Optical MEMS 2001*, vol. IT-7, Sept. 2001.

[7] R. Sawada, E. Higurashi, and A. Shimizu, "Single crystalline mirror actuated electrostatically by terraced electrodes with high aspect ratio torsion spring," in *Proc. IEEE/LEOS Int. Conf. Optical MEMS 2001*, Sept. 2001, pp. 23–24.

[8] H. Toshiyoshi, G.-D. J. Su, J. LaCosse, and M. C. Wu, "Micromechanical lens scanners for fiber optic switches," in *Proc. 3rd Int. Conf. Micro Opto Electro Mechanical Systems (MOEMS'99)*, Mainz, Germany, Aug. 30-Sept. 1, 1999, pp. 165–170.

[9] S. Glockner, R. Goring, B. Gotz, and A. Rose, "Piezoelectrically driven micro-optic fiber switches," *Opt. Eng.*, vol. 37, no. 4, pp. 1229–1234, Apr. 1998.

[10] H. Sankur, R. Hall, E. Motamedi, W. Gunning, and W. Tennant, "Fabrication of microlens arrays by reactive ion milling," in *Proc. SPIE*, vol. 2687, pp. 150–5.

[11] C. R. King, L. Y. Lin, and M. C. Wu, "Out-of-plane refractive microlens fabricated by surface micromachining," *IEEE Photon. Technol. Lett.*, vol. 8, no. 10, pp. 1349–1351, 1996.

[12] H. P. Herzig, *Micro-Optics: Element, System, and Applications*. London, U.K.: Taylor Francis, 1997.

[13] T. Akiyama, D. Collard, and H. Fujita, "Scratch drive actuator with mechanical links for self-assembly of three-dimensional MEMS," *IEEE J. Microelectromech. Syst.*, vol. 6, pp. 10–17, Mar. 1997.

[14] L. Fan and M. C. Wu, "Self-assembled micro-XYZ stages for moving micro-ball lenses," in *Int. Conf. Optical MEMS and Their Applications (MOEMS 97)*, Nara, Japan, Nov. 18–21, 1997, pp. 45–46.

[15] R. T. Chen, H. Nguyen, and M. C. Wu, "A low voltage micromachined optical switch by stress-induced bending," in *Proc. 12th Int. Workshop Micro Electro Mechanical Systems (MEMS 99)*, Orlando, FL, Jan. 17–21, 1999, pp. 424–428.

[16] A. Tuantranont, V. M. Bright, J. Zhang, W. Zhang, J. Ness, and Y. C. Lee, "MEMS-controllable microlens array for beam steering and precision alignment in optical interconnect system," in *Proc. 2000 Solid-State Sensor and Actuator Workshop (Hilton Head 2000)*, Hilton Head Island, SC, June 4–8, 2000, pp. 101–104.

Hiroshi Toshiyoshi (M'97) received the M.Eng. and Ph.D. degrees in electrical engineering from the University of Tokyo, Tokyo, Japan, in 1993 and 1996, respectively.

In 1996, he became a Ph.D. Lecturer with the Institute of Industrial Science (IIS), University of Tokyo. From April 1999 to March 2001, he stayed as a Visiting Assistant Professor at the University of California, Los Angeles. Since September 2001, he has been a Co-Director of IIS's Laboratory for Integrated MicroMechatronic Systems (LIMMS), a joint research group between IIS and the Centre National de la Recherche Scientifique (CNRS), France. Since April 2002, he has been an Assistant Professor of VLSI Design and Education Center (VDEC), attached to the University of Tokyo. His research interest is MEMS for free-space optics and nanomechatronics.

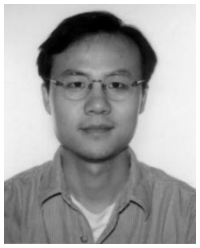

Guo-Dung John Su (M'02) received the B.S. degree from National Taiwan University, Taiwan, in 1992 and the M.S. and Ph.D. degrees in electrical engineering from the University of California, Los Angeles, in 1998 and 2001, respectively.

His doctoral research interest is related to MEMS scanners with flat mirror surface for active optical alignment and micromirror arrays for adaptive optics. Since 2001, he has been with Umachines, Inc., as a Staff Engineer responsible for performing original research as applied to the testing and evaluation of optical components, modules, and interfaces for high-speed fiber optics networking products with integrated MEMS solutions.

Jason Lacosse received the B.S. degree in applied physics from Michigan Technological University, Houghton, and the M.S. degree in electrical engineering from the University of Michigan, Ann Arbor, in 1997.

He is a Product Manager at NP Photonics, Tucson, AZ. He was a Member of the Technical Staff at Boeing after graduation, and was also an Optical Engineer at the Integrated Photonics Laboratory, the University of California, Los Angeles. He has worked in product management since 1999.

Mr. Lacosse is a Member of the Optical Society of America (OSA).

Ming C. Wu (S'82–M'83–SM'00–F'02) received the M.S. and Ph.D. degrees in electrical engineering from the University of California, Berkeley, in 1985 and 1988, respectively.

From 1988 to 1992, he was a Member of the Technical Staff at AT&T Bell Laboratories, Murray Hill, NJ, where he conducted research in high-speed semiconductor lasers and optoelectronics. In 1993, he joined the Faculty of the Electrical Engineering Department of the University of California, Los Angeles, where he is currently a Professor. He is also Director of UCLA's Nanoelectronics Research Facility, and Chair of Photonics and Optoelectronics. His current research interests include MEMS, optical MEMS (MOEMS), microwave photonics, and high-speed optoelectronics. He is also a Member of California NanoSystem Institute (CNSI), one of the four institutes funded by the State of California. He is the Director of the MURI Center on RF Photonic Materials and Devices sponsored by ONR. He has published over 110 journal papers, 200 conference papers, contributed one book chapter, and holds eight U.S. patents.

Dr. Wu was General Co-Chair of the IEEE LEOS Summer Topical Meeting in 1995 (RF Optoelectronics), 1996 and 1998 (Optical MEMS), and 1999 International Conference on MOEMS. He has also served on the Program Committees of OFC, CLEO, MEMS, Optical MEMS, IEDM, and DRC. He received the Packard Foundation Fellowship in 1992. He is a Member of the American Physical Society, Optical Society of America (OSA), URSI, and Eta Kappa Nu.